American Mineralogist, Volume 62, pages 1225–1231, 1977

Natural alteration of vermiculite to chrysotile

AMPARO MIFSUD, VICENTE FORNES AND JOSE A. RAUSELL-COLOM

Instituto de Edafología y Biología Vegetal, C.S.I.C.
Serrano 115-dup, Madrid-6, Spain

Abstract

A topotactic alteration of vermiculite to chrysotile has been observed in spotted vermiculite samples from Kapirikamodzi, Malawi. The identification of the alteration material as chrysotile is based on evidence furnished by X-ray diffraction, IR spectroscopy, and selected-area electron diffraction. Transmission and high-resolution electron photomicrographs provide grounds for the interpretation of the alteration process as topotactic in nature. A mechanism is proposed by which the transformation could possibly be accomplished under the mild hydrothermal conditions which seem to have prevailed during the genesis of the vermiculite.

Introduction

While investigating the properties of several vermiculites, we noticed on a hand specimen of brown vermiculite from Kapirikamodzi, Malawi, the existence of small spots of a silvery color (Fig. 1). This suggested some kind of alteration, whose nature was thought worth investigating.

The Kapirikamodzi basement (Fig. 2) is a hill about 4000 feet long and 1500 feet wide, consisting of a core of a soft decomposed rock made up almost entirely of vermiculite flakes with occasional residual patches of black hydrobiotite. The core is ramified by quartz-microcline pegmatites and magnesite veins, and is bordered by biotitite rock (Morel, 1955).

Two main types of vermiculite are found in the basement: (a) the main-body vermiculite, consisting of flakes of about 1 to 6 mm; (b) massive honey-yellow crystals, up to 20 cm in diameter and 5 cm thick, which only occur at the margins of quartz–feldspar pegmatites that ramify the vermiculite rock. The specimen investigated here belongs to this second type.

According to Morel (1955) the fine-grained material of the main body was formed from the original biotitite rock, now surrounding the basement, which was altered to vermiculite as a result of pegmatitic intrusions through the operation of magmatic fluids. The large books of the second type, however, are described as "pegmatitic" vermiculite, *i.e.*, vermiculite formed by reaction at the contact zone between the acidic intrusions and ultrabasic peridotite rock that formerly underlaid the basement.

Sample preparation

Small vermiculite flakes were cleaved from zones of the specimen which were visually free from silvery spots, and also from other zones where those spots were more abundant. Each lot was ground, dispersed in water, and the fraction of less than 5μ (*e.s.d.*) was separated by centrifugation. A few grams were taken from the fine fraction of each lot and were saturated

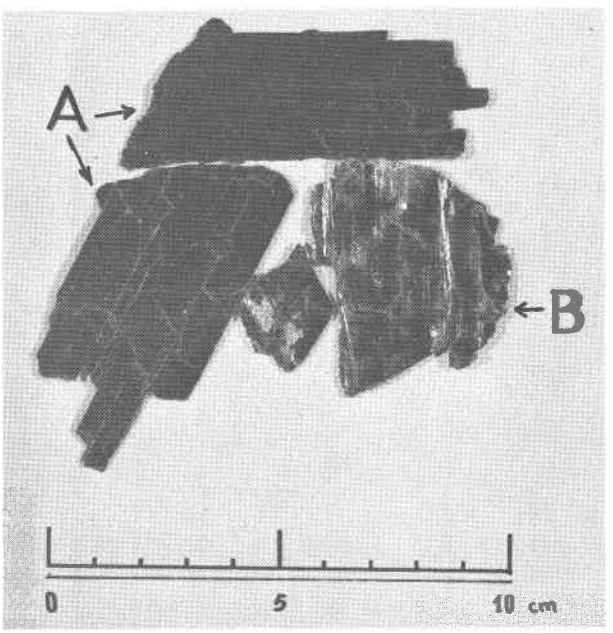

Fig. 1. Photograph showing vermiculite specimens: (a) unaltered, (b) with altered silvery spots.

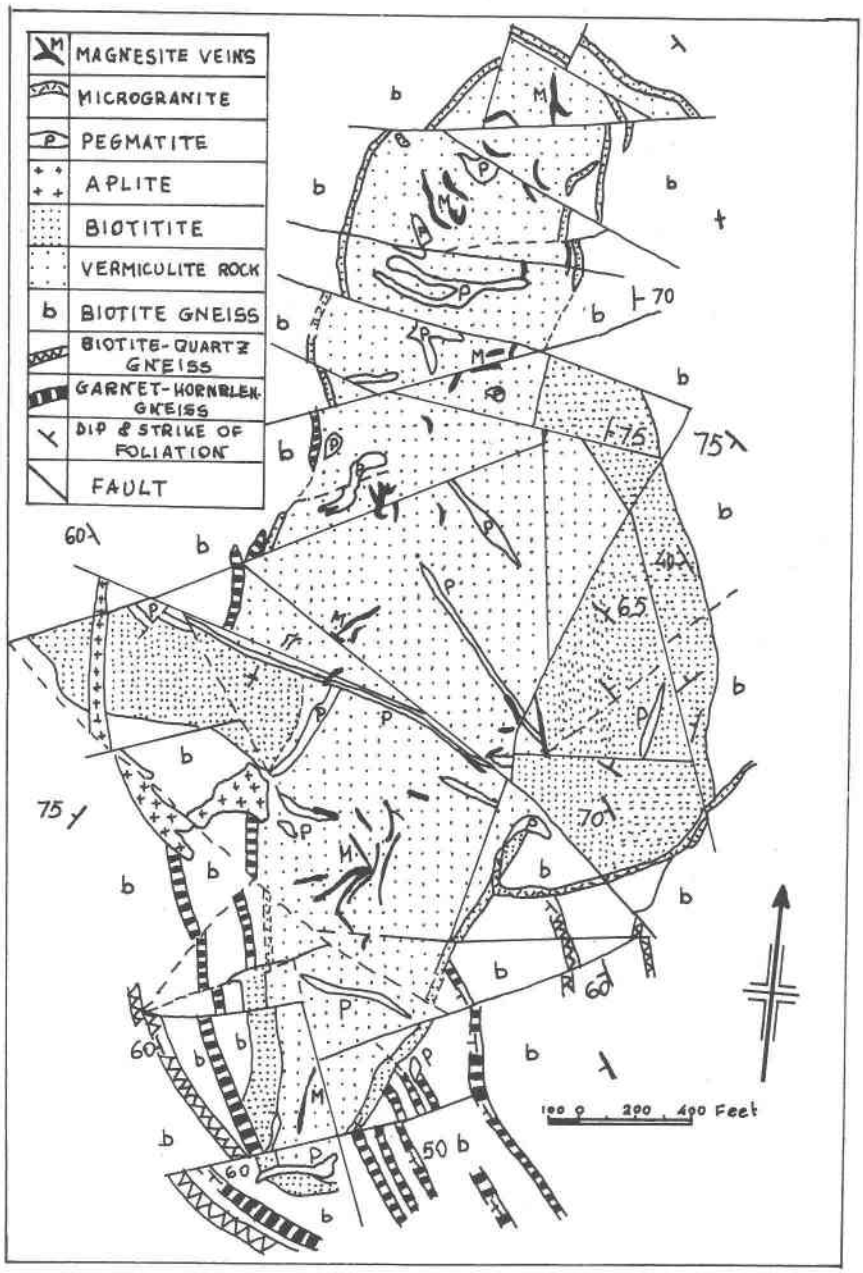

Fig. 2. Geological map of the Kapirikamodzi complex; after Morel (1955).

with calcium by treatment with 0.5N $CaCl_2$. The two specimens were washed free of excess Cl^- and calcinated to 1000°C. Elemental analyses by X-ray fluorescence spectroscopy were made on these specimens.

From the fine fraction separated from the flakes rich in silvery spots, specimens were prepared for X-ray diffraction, IR spectroscopy, transmission and high-resolution electron microscopy, and selected-area electron diffraction.

Oriented aggregates (2–4 mg/cm²) were used for X-ray diffraction. These were prepared from the natural, Mg-saturated material and also from material previously saturated with barium. KBr disks were used for IR spectroscopy. A diluted vermiculite-water suspension was shaken in an ultrasonic vibrator, and specimens were prepared for transmission electron microscopy and selected area electron diffraction in the usual way. For high-resolution electron

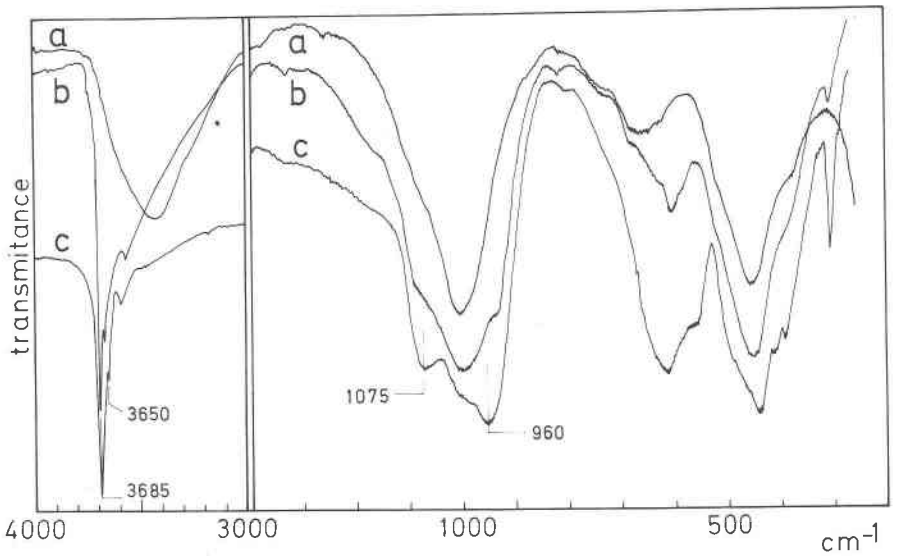

Fig. 3. Infrared absorption spectra: (a) vermiculite (unaltered), (b) vermiculite (altered), (c) chrysotile from Ronda, Spain.

microscopy ultrathin sections were obtained by the technique described by Tchoubar *et al.* (1973).

IR spectroscopy

Figure 3 shows IR spectra of the pure vermiculite (*a*), of the spotted vermiculite (*b*), and of natural chrysotile (*c*). It is apparent that spectrum *b* contains bands characteristic of both vermiculite and chrysotile. Thus, sharp bands at 3685 and 3650cm^{-1} in the OH stretching region are characteristic of chrysotile. Similarly in the Si–O region two bands at 1075 and 960cm^{-1}, characteristic of chrysotile, appear as shoulders overlapping the broad band of vermiculite at 1000 cm^{-1}

X-ray diffraction diagrams

Figure 4 gives X-ray diffraction diagrams of oriented aggregates of the spotted vermiculite (Mg-saturated and Ba-saturated) at room temperature and after heating at 530° and 620°C. In Figure 4a the presence of two crystalline phases, one of d_{001} = 14.3 A (Mg-vermiculite) and a second of d_{001} = 7.3 A (chrysotile) is apparent. On the diagram of the barium-saturated specimen (Fig. 4b), the overlap of the peaks of the two phases is avoided since the d_{001} peak of vermiculite has shifted to 12.3 A, leaving the chrysotile peaks at 7.3 and 3.64 A unaffected. On heating at 530° the intensity of these two peaks decreases considerably (Fig. 4c), and at 630°C the chrysotile phase is totally destroyed (Fig. 4d).

Electron microscopy and selected area diffraction

Figure 5 shows transmission electron photomicrographs of vermiculite particles at different stages of alteration. In Figure 5a, tears have developed on the

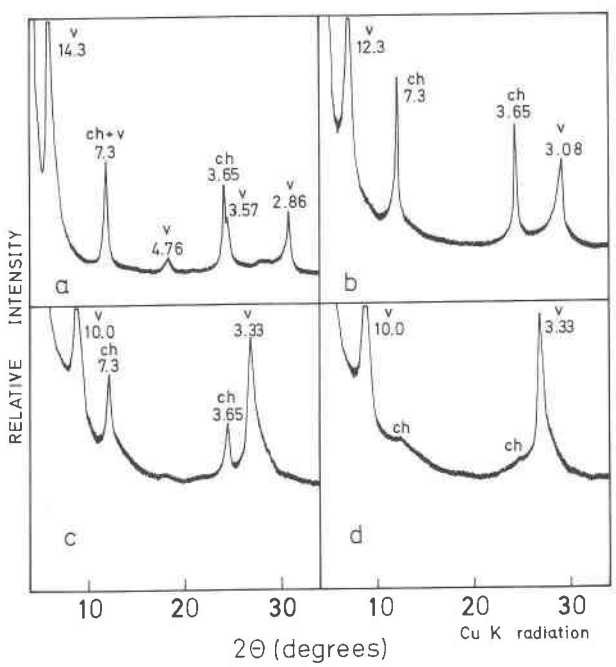

Fig. 4. X-ray diffraction diagrams of oriented aggregates of altered vermiculite, fine fraction (<5μ): (a) Mg-saturated; (b) Ba-saturated; (c) Ba-saturated, heated 4 hr at 530°C; (d) Ba-saturated, heated 4 hr at 620°C.

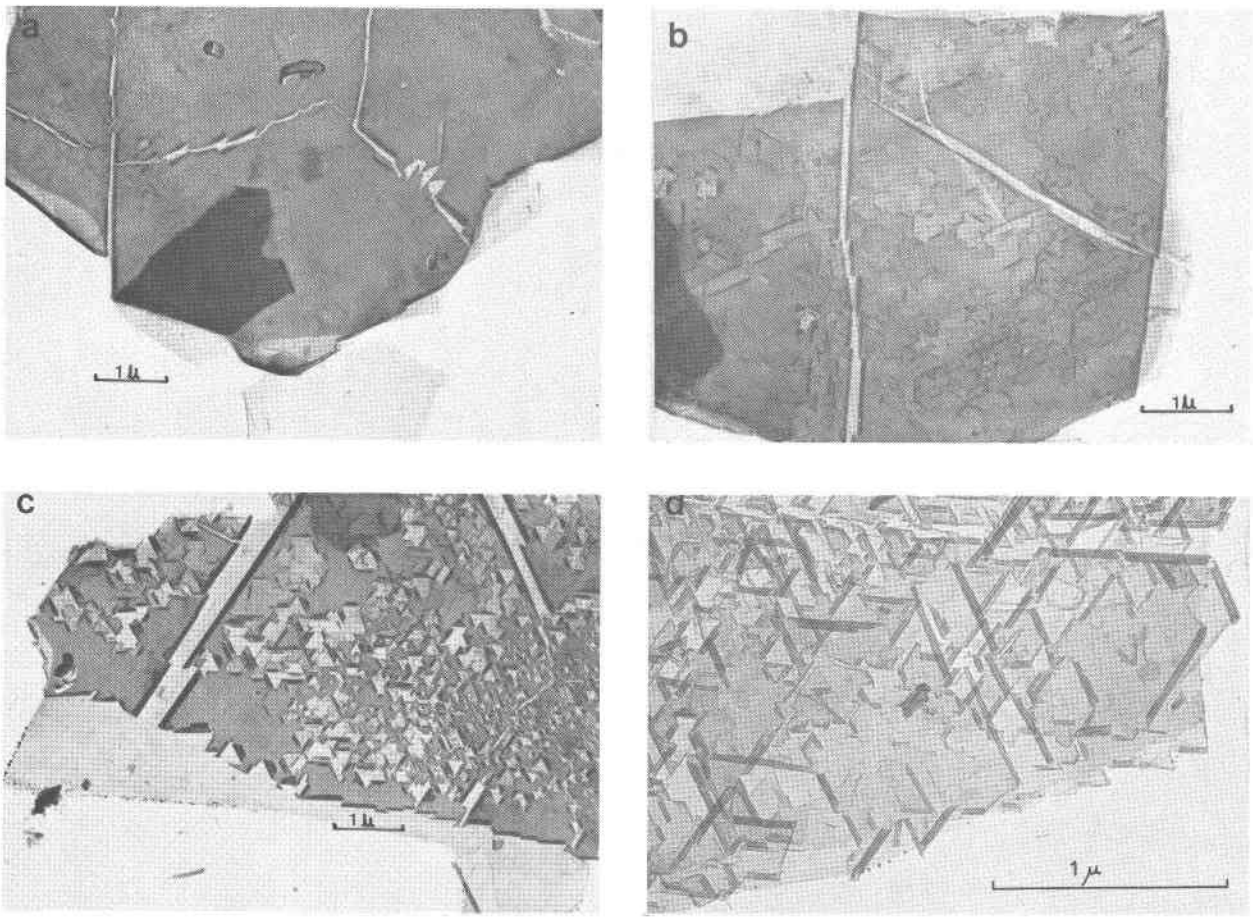

Fig. 5. Transmission electron photomicrographs of vermiculite particles at different stages of alteration: (a) tearing of top layers of the vermiculite plates; (b) and (c) two stages of the development of elongated crevices and polygonal pits, with folded vermiculite ribbons at their edges; (d) chrysotile tubes formed at places where folded vermiculite ribbons had developed.

surfaces of the vermiculite plates, along which one sees occasionally thin vermiculite layers folded back upon themselves. The nature of such folding is revealed in cross-section in Figure 6a. Figures 5b and 5c show the occurrence of this folding to a greater extent, and in addition, one sees polygonal areas where the vermiculite plates are thinner than at the surrounding portions, and from which similar folding has also occurred. Finally, in Figure 5d hollow tubes or scrolls having the morphological features of chrysotile are seen in places where folded vermiculite ribbons had formed.

The chrysotile particles are about 0.02μ in diameter and from 0.2 to 1μ in length and are arranged in an orderly manner, either parallel or at angles of 60° or 120° degrees from each other, as were the folded vermiculite ribbons of Figures 5b and 5c. Furthermore, selected-area diffraction patterns have been taken where the diffraction from vermiculite and from the chrysotile overlap. They indicate that the long direction of the fibers coincides with the 100, $\bar{1}30$, and $\bar{1}\bar{3}0$ crystallographic direction of vermiculite plates.

At still higher magnification (Fig. 7a) most of the particles exhibit a polygonal rather than a cylindrical morphology, a feature that has already been recognized for certain chrysotiles (Maser *et al.*, 1960). This is better illustrated in Figure 6b, reproducing a high-resolution electron photomicrograph of a thin cross-section parallel to the *c* axis of the vermiculite platelet and normal to the *a* axis of the chrysotile needle.

A selected-area electron diffraction micrograph from an isolated tube (Fig. 7b) shows diffraction spots distributed along layer lines of 5.3 A periodicity in the direction of the fiber axis. It mainly contains $h0l$ and $h0\bar{l}$ reflections, grouped in pairs, and also some $hk0$ reflections, all corresponding to a cylindrical lattice with $a = 5.3$, $b = 9.2$, $c = 14.6$A, $\beta =$

93°, such as that of the clinochrysotile cell (Zussman *et al.*, 1957). The splitting of some *hk* reflections into triplets can be noticed. This feature is characteristic of electron diffraction diagrams of some chrysotiles and indicates the existence within the fiber of several crystalline domaines at slightly different orientations (Zviagin, 1967).

Analytical data

Table 1 gives the chemical analyses, based on Ca-saturated ignited material. Table la corresponds to the vermiculite devoid of chrysotile, and Table 1b to the mixture of the two mineral species. The figure for the CaO content would correspond, in the natural material, to the interlayer exchangeable Mg content of the vermiculite phase. Comparison of the two analyses shows clearly that the alteration of part of the vermiculite into chrysotile involves primarily a substantial loss of Fe and a gain in Mg. Therefore, one may expect the composition of the new phase formed to approach the composition of an Al-rich chrysotile (Deer *et al.*, 1962).

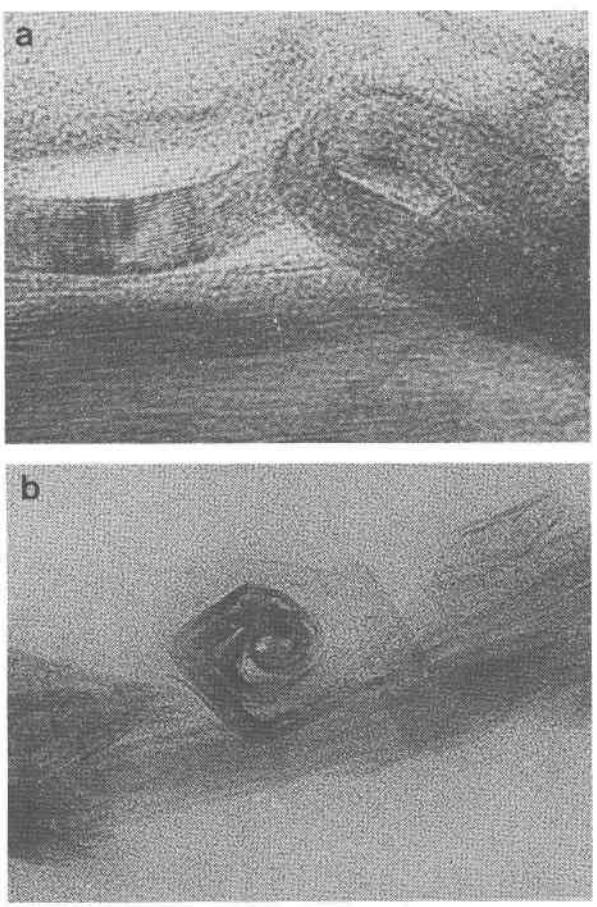

Fig. 6. High-resolution electron photomicrographs of (a) thin cross-section of a vermiculite platelet with rims folded on either side of a surface crack, (b) thin cross-section of vermiculite platelet with attached chrysotile fiber.

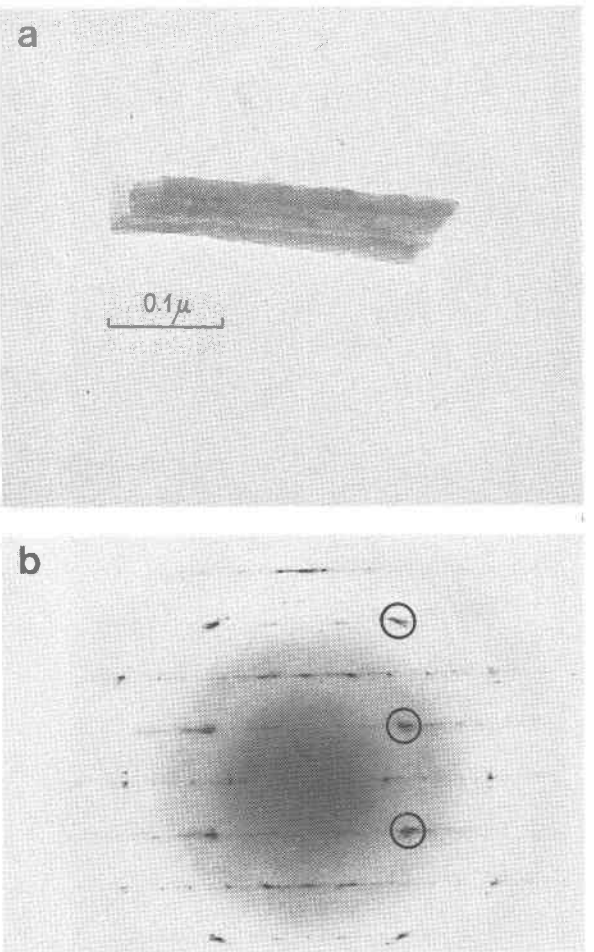

Fig. 7. Isolated fiber of chrysotile: (a) electron photomicrograph, (b) selected-area electron diffraction pattern.

Discussion

From the evidence presented above, the identification as chrysotile of the mineral phase accompanying vermiculite in this particular specimen seems sufficiently accomplished. It is also apparent from the electron photomicrographs that the material making up the chrysotile tubes was torn from the top layers of the vermiculite plates at places where the elongated crevices and polygonal pits are now seen, and which are thinner in depth than the rest of the plate. Therefore, it can be concluded that despite the orderly disposition of the chrysotile particles, one is not dealing with some sort of epitaxial growth on the ver-

Table 1. Chemical analyses*

	a	b
SiO_2	43.82	45.27
Al_2O_3	13.42	13.20
Fe_2O_3	7.81	5.00
MnO	0.06	0.04
TiO_2	1.21	1.18
MgO	26.82	28.47
K_2O	0.00	0.02
CaO	4.87	5.48
Na_2O	n.d.	n.d.
TOTALS	98.01	98.66

a. unaltered vermiculite
b. vermiculite from altered silvery spots

**estimated precision of chemical analyses: maximum error 1 per cent relative*

miculite substrate, but rather with a topotactic alteration of the vermiculite itself. First, surface cracks are developed along well-defined crystallographic directions (Si–O–Si chains). Next, the vermiculite folds back at the edges of the cracks. Finally, the looser folded vermiculite ribbons or scrolls are transformed into chrysotile, undergoing chemical changes mainly by a removal of Fe and an enrichment in Mg and OH.

The alteration of phlogopite to a serpentine mineral phase has been reported by Roy and Romo (1957), and similar chemical changes may be inferred. Also, analogous morphological changes have been observed when Fe-rich vermiculites have been treated in the laboratory with concentrated salt solutions at elevated temperatures (Roth *et al.*, 1966). The fact that, in the present instance, the final alteration product is chrysotile would indicate alteration by Mg-bearing hydrothermal solutions rather than by surficial weathering.

Structurally the conversion of vermiculite into chrysotile seems feasible, as Figure 8 shows. This requires the extraction of Al and Fe from the tetrahedral sheet and the replacement of Fe by Mg in the octahedral sheet in the talc-like layers, the introduction of more Mg and OH in the interlayers, and the reversal of one of the Si–O sheets towards the newly formed "brucite" layer. This involves breaking Si–O–Mg bonds and inverting the SiO_4 tetrahedra, and requires rejecting water ahead of the crystallization. It is not known what the energy requirements for this transformation reaction would be, but they could possibly be accounted for by the mild hydrothermal conditions that can be expected from pegmatitic fluids permeating an ultrabasic rock, *i.e.*, the conditions that prevailed when the vermiculite was formed (Morel, 1955).

As far as the authors are aware, this is the first reported example of vermiculite altering topotactically into chrysotile.

Acknowledgments

The authors are indebted to Dr. J. Galvan from the Laboratory of Electron Microscopy, Instituto de Edafologia y Biologia Vegetal (CSIC), Madrid, for transmission electron photomicrographs, to Dr. M. Rautureau, from CRSOCI (CNRS), Orleans, France, for the high-resolution electron photomicrographs, and to Dr. K. Norrish from the Division of Soils (CSIRO), Adelaide, Australia, for the chemical analyses.

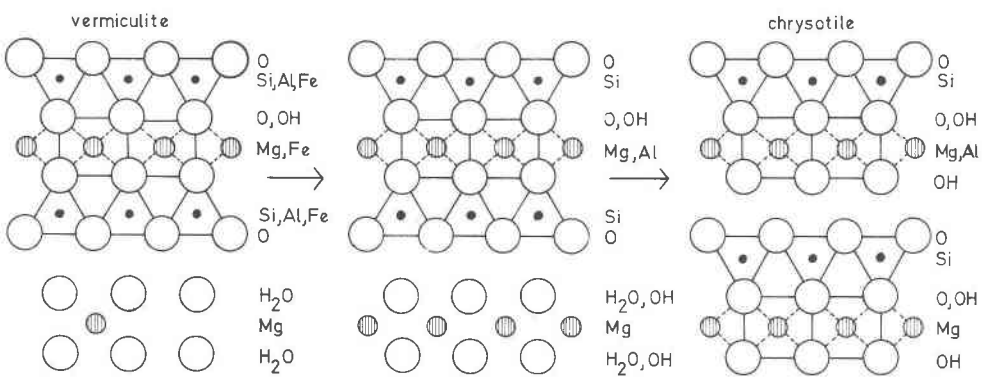

Fig. 8. Diagramatic representation of compositional and structural changes involved in the alteration of vermiculite to chrysotile.

References

Deer, W. A., R. A. Howie and J. Zussman (1962) *Rock Forming Minerals*, Vol. 3, *Sheet Silicates*. John Wiley and Sons, New York.

Maser, M., R. V. Rice and H. P. Klug (1960) Chrysotile morphology. *Am. Mineral., 45,* 680–688.

Morel, S. V. (1955) Biotitite in the basement complex of Southern Nyasaland. *Geol. Mag., 92,* 241–254.

Roth, C. B., M. L. Jackson, J. M. de Villiers and V. V. Volk (1966) Surface colloids of micaceous vermiculite. *Trans. Comm. II&IV Int. Soc. Soil Sci., Aberdeen,* 217–221.

Roy, R. and L. A. Romo (1957) Weathering studies. I. New data on vermiculite. *J. Geol., 65,* 603–610.

Tchoubar, C., M. Rautureau, C. Clinard et J. P. Ragot (1973) Technique d'inclusion appliquée á l'étude des silicates lamellaires et fibreux. *J. Microscopie, 18,* 147–154.

Zussman, J., G. W. Brindley and J. J. Comer (1957) Electron diffraction studies of serpentine minerals. *Am. Mineral., 42,* 133–153.

Zviagin, B. B. (1967) *Electron Diffraction Analysis of Clay Minerals Structures*. Plenum Press, New York.

Manuscript received, May 12, 1977; accepted for publication, July 8, 1977.